Fate of pairing and spin-charge separation in the presence of long-range antiferromagnetism

Luhang Yang, Ignacio Hamad, Luis O. Manuel, and Adrian E. Feiguin

The fate of pairing and spin-charge separation in the presence of long-range antiferromagnetism

Luhang Yang,[1] Ignacio Hamad,[2] Luis O. Manuel,[2] and Adrian E. Feiguin[1]

[1]*Department of Physics, Northeastern University, Boston, Massachusetts 02115, USA*
[2]*Instituto de Física Rosario (CONICET) and Facultad de Ciencias Exactas, Ingeniería y Agrimensura, Universidad Nacional de Rosario, Rosario, Argentina*

We present a numerical study of competing orders in the 1D t-J model with long-range RKKY-like staggered spin interactions. By circumventing the constraints imposed by Mermin-Wagner's theorem, this Hamiltonian can realize long-range Néel order at half-filling. We determine the full phase diagram as a function of the exchange and particle density using the density matrix renormalization group (DMRG) method. We show that pairing is disfavored and the AFM insulator and metallic phases are separated by a broad regime with phase segregation, before spin-charge separation re-emerges at low densities. Upon doping, interactions induce a confining potential that binds holons and spinons into full fledged fermionic quasi-particles in a range of parameters and densities. We numerically calculate the photoemission spectrum of the model, showing the appearance of a coherent quasi-particle band splitting away from the holon-spinon continuum with a width determined by J that survives at finite doping. Comparison with analytical results using the self-consistent Born approximation (SCBA) and by solving the spinon-holon problem offer insight into the internal structure of the quasi-particles and help us explain the different features in the spectrum. We discuss how this simple toy-model can teach us about the phenomenology of its higher dimensional counterpart.

I. INTRODUCTION

Understanding the properties of doped antiferromagnets has been a topic of great theoretical interest for the past few decades[1, 2]. This is motivated by the lack of a universal theory of high-temperature superconductors that can explain the mechanisms behind the formation of Cooper pairs in this kind of materials, where strong electronic correlations are assumed to play a dominant role. Most of the research in this area has been focused on the study of paradigmatic simple model Hamiltonians that are supposed to capture all the basic ingredients for high temperature superconductivity such as the Hubbard and $t-J$ models and variations of them[1, 3–7]. In this context, much effort has been devoted to their low-dimensional versions[8–26]. Particularly, in one dimension the physics of these systems can be universally described in the framework of Luttinger liquid (LL) theory[27–32]: the natural excitations in 1D are described in terms of spin and charge excitations that propagate coherently with different velocities and are characterized by distinct energy scales, leading to the concept of spin-charge separation. The spectrum of a spin-full LL is determined by a convolution of the spin and charge spectra, which leads to a continuum without well defined Landau quasi-particles and Fermi-edge singularities instead of quasi-particle peaks[33, 34]. Interestingly, the Hubbard model in 1D admits an exact solution in terms of the Bethe ansatz [35–37], and the $t-J$ model also realizes an exactly soluble "supersymmetric" point at $J/t = 2$[38–42], allowing one to infer information about the nature of the excitations.

An important difference between one and two dimensions is established by the Mermin-Wagner theorem[43, 44]: at zero temperature, gapless one-dimensional local Hamiltonians cannot realize long-range order, while two dimensional systems can display spontaneous symmetry breaking. At half-filling, where the physics can be more easily understood in the context of the Heisenberg model, the ground state of a 1D chain is a spin-liquid with algebraically decaying correlations and domain-wall-like spin excitations (spinons) that carry spin $S = 1/2$. On the other hand, the ground state in two dimensions displays Néel order, and excitations are magnons that condense into Goldstone modes.[45]

Besides the omnipresent question concerning the role of antiferromagnetism as a glue for pairing, a more basic and fundamental one has also remained central to the problem: is it possible for spin-charge separation to survive in two dimensions? [46–65]. Alternatively, one can postulate the opposite question: What is the fate of spin charge separation in the presence of long-range antiferromagnetic order? The spin-charge separation phenomenon is usually considered as a manifestation of 1D physics, and whether it exists in higher dimensions is a topic of debate, especially in the context of understanding high-Tc superconductivity[55] and recent experiments in cold-atom systems[66–82]. Over the past decades it has become quite clear that a definitive answer to these questions can only be obtained numerically. Unfortunately, quantum Monte Carlo (QMC) has not been able to provide evidence since calculations are carried out at finite temperature and with the use of difficult to control analytic continuation[83–86]. At the same time, the success of the density matrix renormalization group method (DMRG) [87, 88] and tensor networks has only partially extrapolated to two dimensions[89–92].

One possible avenue to circumvent these hurdles and study the dimensional crossover consists of introducing long-range interactions in one-dimension since[93–99]: (i)
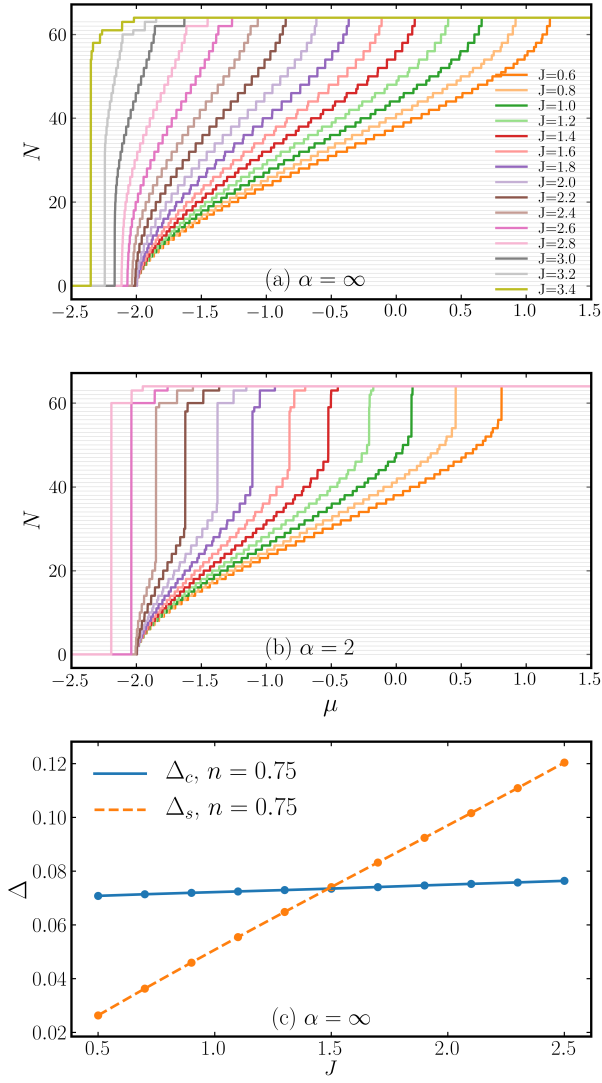
FIG. 1. Particle number as a function of chemical potential for the (a) conventional $t-J$ model ($\alpha = \infty$) and (b) $\alpha = 2$ for several values of J in descending order from left to right.(c) Charge and spin gaps for a conventional $t - J$ chain with $L = 64$ sites.
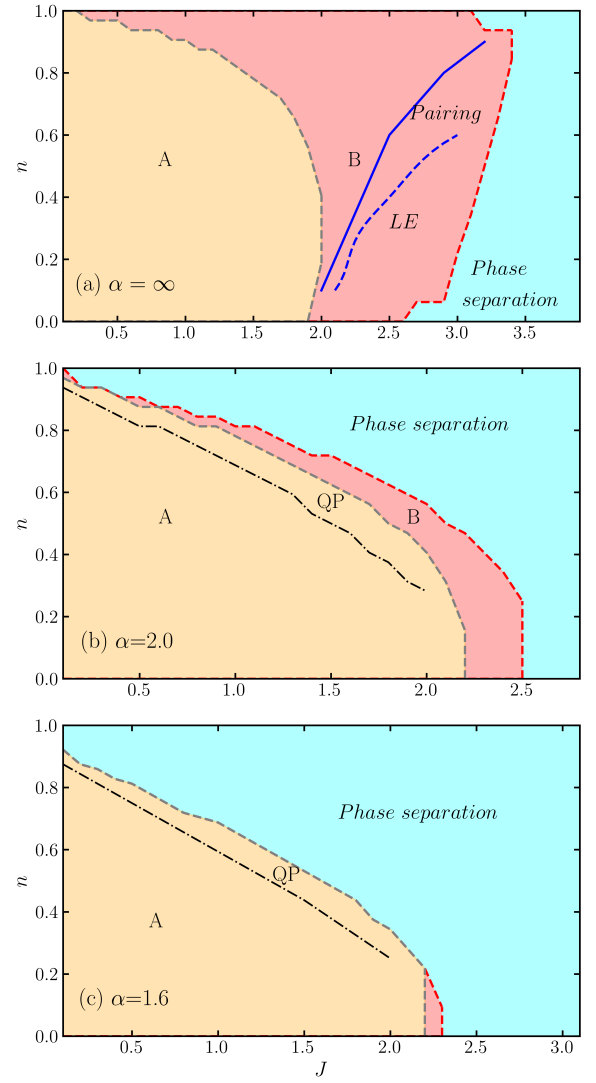

FIG. 2. (a) Phase diagram of the conventional $t - J$ chain. Regions A and B represent regimes where the occupation changes by $\Delta N = 1$ and $\Delta N = 2$ with varying the chemical potential, respectively. The solid and dashed blue curve are the phase boundaries of the paired and Luther-Emery phase, respectively. (b)-(c) Phase diagrams for the $t - J$ chain with long range spin interactions and (b) $\alpha = 2$ and (c) $\alpha = 1.6$. The dotted-dashed line indicates the boundary between phase separation and fermionic quasiparticles (see text). All results are for a chain with $L = 64$ sites.

they effectively increase the dimensionality of the problem through all-to-all interactions; (ii) overcome the limitations of Mermin-Wagner theorem allowing one to probe for true long range order and spontaneous symmetry breaking; (iii) they offer a relatively simple and intuitive playground where to test for higher dimensional physics within the reach of powerful numerical techniques such as the DMRG method.

In this work, we focus on understanding the role of long range interactions in a doped one-dimensional antiferromagnet using an extended $t - J$ model with RKKY-like AFM long-range interactions:

$$H = H_{t-J} + H_{RKKY} \qquad (1)$$

$$H_{t-J} = -t \sum_{i\sigma}(c^{\dagger}_{i,\sigma}c_{i+1,\sigma} + h.c.) \qquad (2)$$

$$+ J \sum_{i}(\vec{S}_i \cdot \vec{S}_{i+1} - \frac{1}{4}n_i n_{i+1})$$

$$H_{RKKY} = \lambda \sum_{i,j>i+1} \frac{(-1)^{j-i+1}}{|j-i|^{\alpha}}(\vec{S}_i \cdot \vec{S}_j), \qquad (3)$$

where the operator $c^{\dagger}_{i\sigma}$ creates an electron on site i along the chain with spin $\sigma =\uparrow,\downarrow$, n_i is the electron number
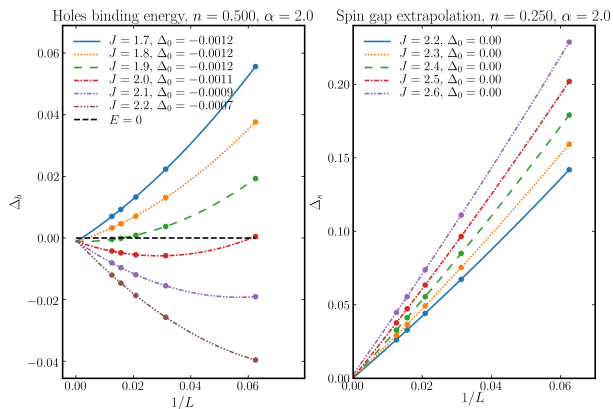
FIG. 3. Left panel: binding energy between two holes, extrapolated to the thermodynamic limit with second order polynomial fit for $n = 0.5$, $\alpha = 2$. The exchange J varies through region B in phase diagram Fig.2(b). Right panel: spin gap extrapolated to thermodynamic limit with second order polynomial fit obtained with DMRG for density $n = 0.25$ and $\alpha = 2$; the exchange J ranges from metallic phase to the phase separation boundary.

operator, $\vec{S}$ represents spin $S = 1/2$ operators. The constants J and λ parametrize the magnitude of the spin exchange and RKKY interactions that decay as a power law with exponent α. In the rest of the paper and for simplicity, we focus on the case $\lambda = J$ and we study finite chains of length L. The $t - J$ model describes the low-energy physics of the Hubbard model when the Coulomb repulsion is very large compared to the hopping constant t, that we take as our unit of energy. In this context, a constraint forbidding double-occupancy is implicitly assumed.

The quantum phase diagram of conventional $t - J$ model in 1D has been extensively studied[100, 101]. At half-filling, this Hamiltonian reduces to the one-dimensional Heisenberg chain. Upon doping and for large J, spins prefer to form antiferromagnetic domains and clump together phase separating into electron-rich and hole-rich regions. In the metallic phase with $J/t < 2$, the low energy physics can be well described in terms of Luttinger liquid theory. In this phase, the low energy excitations are holons carrying charge with characteristic velocity v_h and a bandwidth determined by the hopping t, and spinons carrying spins with velocity v_s and a bandwidth proportional to J.

In addition to the Luttinger liquid metallic phase, in the intermediate J/t range the $t - J$ model exhibits a Luther-Emery regime at low densities with a spin gap and dominant pairing correlations and a superconducting phase at high densities between the metallic LL phase and phase separation (See Fig.2(a)).

One can in principle assume that the origin of the RKKY term can be the proximity to a two dimensional layer with long range antiferromagnetic order[63]. Notice that the sign of the interactions alternates between anti-

ferro and ferromagnetic depending on the sublattice and it enhances the tendency of the spins to antiferromagnetically align. At half-filling, this translates into a regime with spontaneous symmetry breaking and long range order for α small enough $\alpha < 2.2$[94]. While the elementary excitations of the Heisenberg chain are deconfined domain-wall-like spinons, an effective confining potential emerges as a consequence of the long-range interactions that binds spinons together to form coherent magnon-like gapless excitations above the antiferromagnetic ground state. In this work, we aim at describing and understanding how similar effects can alter the spin-charge separation picture and induce confinement between spinons and holons such that they bind forming composite quasi-particle states that carry both, spin and charge degrees of freedom. Moreover, we observe that with these modifications to the $t - J$ model, excitations will no longer display a linear dispersion at the Fermi level and LL theory will not apply in its conventional formulation[102].

This paper is organized as follow: firstly we study the quantum phase diagram for $t - J$ chain with long range spin couplings and show the dominant orders in different phases in sec.II. In sec.III we discuss the stability of composite quasi-particles using energetic considerations. We support this evidence by means of numerical and analytical calculations of the spectral function for a single hole in sec.IV using DMRG, the self-consistent Born approximation (SCBA) and by solving the spinon-holon problem. We extend these considerations to finite doping in sec.V. We finally close with a summary and discussion of the results.

II. PHASE DIAGRAM

In order to determine the quantum phase diagram of the model, we use the DMRG method with open boundary conditions to calculate the ground state energies $E_0(J, N)$ by varying J in steps of 0.1 and changing the total particle number N between 0 and L, where L is the length of the chain. In all calculations we chose the bond dimension such that the truncation error is always below 10^{-6}. Interestingly, despite the long range interaction, we observe that the entanglement does not grow dramatically, allowing us to maintain all sources of error under control (basically, by using enough DMRG states). We use the Maxwell construction to obtain the N versus chemical potential μ curves and determine the stable ground state densities, as shown in Fig.1 (basically, for a fixed chemical potential μ, the corresponding density is determined by the minimum of $E_0 - \mu N$). For validation, we include results for the conventional $t - J$ chain of length $L = 64$. We can identify different behaviors in terms of how the density N jumps from one value to the next as μ is varied. One can distinguish three regimes, summarized in the phase diagram Fig.2(a): (i) a metallic phase where the occupation changes in steps of one particle ($\Delta N = 1$) labeled as "A"; (ii) a region "B" where it
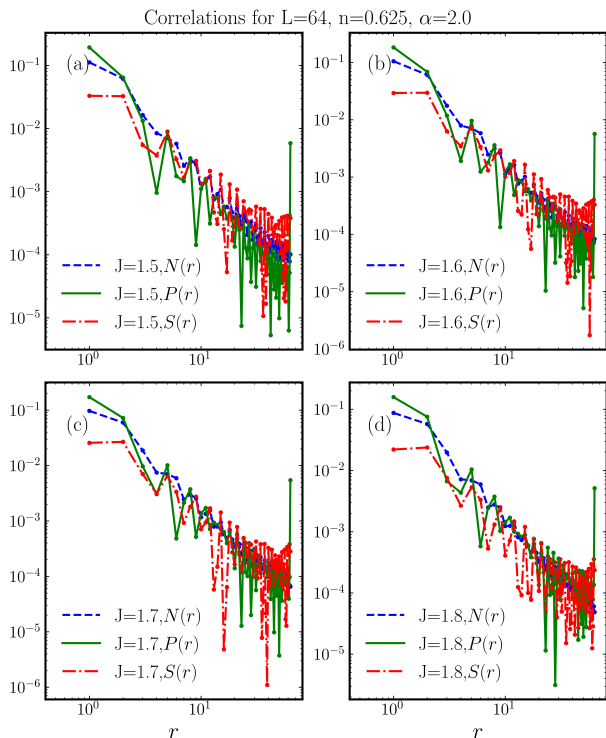
FIG. 4. Singlet pair-pair, density-density, and spin-spin correlations in real space for $L = 64$, $n = 0.625$, and $\alpha = 2$. J varies through region B in phase diagram Fig.2(b)
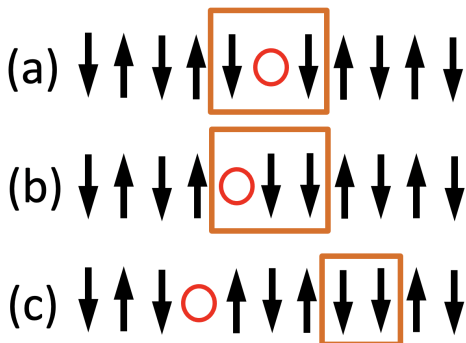

FIG. 5. Cartoon picture in the Ising limit illustrating: (a) A confined holon and spinon pair; (b) a spinon a distance $r = 1$ from the holon, still forming a bound pair; (c) deconfined spinon and holon. The box highlights the position of the spin domain wall.

changes in steps of two ($\Delta N = 2$); and finally (iii) the occupation abruptly jumps between an intermediate value and $n = N/L = 1$. This sudden change is associated to phase segregation: for large J the system splits between hole-rich regions and domains with density $n = 1$ and AFM correlations. The steps $\Delta N = 2$ can be interpreted as an indication of pairing. However, it turns out that an alternative explanation is possible: due to spin-charge separation, the creation of a hole translates into the excitation of both a spinon and a holon that, as we

mentioned, have characteristic velocities v_s and v_h. This means that in the regime with $v_s > v_h$ it is energetically more favorable to create two holons without exciting any spinons, rather than a single holon and a spinon[42, 103]. This is expected to occur for large enough J, which is precisely where this is observed in the phase diagram. To support this argument, we define the singlet-triplet spin gap:

$$\Delta_s = E(N, S^z = 1) - E(N, S^z = 0)$$

and the charge gap:

$$\Delta_c = E(N + 1, S^z = 1/2) + E(N - 1, S^z = 1/2) \\ - 2E(N, S^z = 0). \quad (4)$$

In Fig.1(c) we show both quantities for $L = 64$ and density $n = N/L = 0.75$. As one can see, the charge gap has a very weak dependence on J and is essentially determined by the level spacing $\Delta_c \sim 4t/L = 0.0625$. Both gaps extrapolate to zero in the $L \to \infty$ limit (not shown) but in finite systems they display a crossing at precisely the value of J where the steps change from $\Delta N = 1$ to $\Delta N = 2$. Hence, this is a finite-size effect since both spinons and holons are gapless in the thermodynamic limit. However, it is a feature that should remain observable in finite chains and can help us as a guide in our search for pairing, since that should also manifest itself as steps $\Delta N = 2$ as well. As a matter of fact, pairing is known to be stable in this regime [101], as shown in the same figure. There are two distinct paired phases: a gapless one with algebraically decaying but dominant pair-pair correlations, and a spin-gapped Luther-Emery phase.

In Figs.2(b) and (c) we show similar phase diagrams for the $t - J$ model with long-range RKKY interactions and for two values of exponent $\alpha = 1.6, 2.0$. We firstly recall that at half-filling the system undergoes a transition from spin liquid for large α to Néel AFM for small α at a value of $\alpha_c \sim 2.2$. The long-range interaction plays the role of enhancing the AFM order. As a consequence, upon doping with holes, electrons tend to clump together in a large ordered domain, displacing the holes toward the boundaries of the chain. Therefore, smaller alpha translates into a growing phase separated region that dominates the phase diagram, also pushing the metallic phase to lower densities. On the other hand, at a value of $\alpha = 2$ close to the transition we see that the $\Delta N = 2$ regime survives albeit in a much narrower window. However, pairing does not survive. To show this, we calculate the pair binding energy describing the energy gain for creating a pair of holes

$$E_b = (E_{2holes} - E_0) - 2(E_{1hole} - E_0) \\ = E_0 + E_{2holes} - 2E_{1hole}, \quad (5)$$

where we have defined $E_{2holes} = E(N = L - 2, S^z = 0)$; $E_{1hole} = E(N = L - 1, S^z = 1/2)$ and $E_0 = E(N = L, S^z = 0)$. Finite size extrapolations of Δ_b and the spin
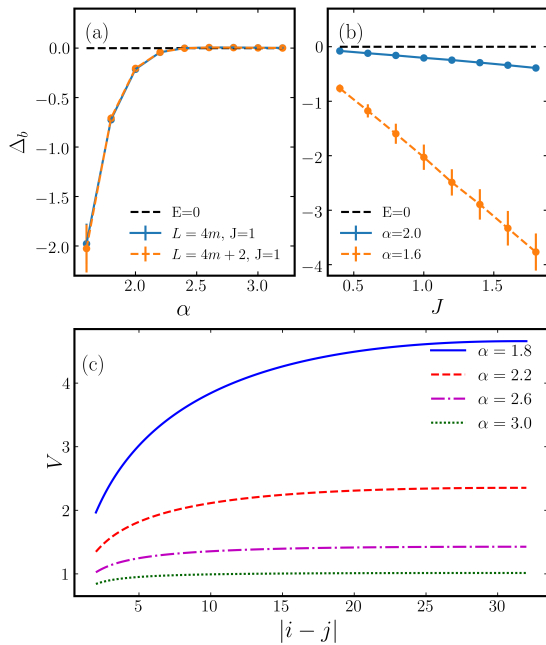
FIG. 6. Binding energy between holon and spinon as a function of (a) α for fixed $J = 1$ and (b) as a function of J for different values of α, extrapolated to the thermodynamic limit using chains of lengths $L = 4m$ and $L = 4m + 2$ (see text). (c) Confining potential between holon and spinon in the Ising limit.

gap Δ_s are shown in Fig.3 clearly indicate that both are zero in the thermodynamic limit within our error bars.

To offer more insight into this issue, we also calculate the spin-spin correlation:

$$S(r) = \langle S_0^z S_r^z \rangle, \tag{6}$$

density-density correlation:

$$N(r) = \langle n_0 n_r \rangle - \langle n_0 \rangle \langle n_r \rangle \tag{7}$$

and pair-pair correlation:

$$P(r) = \langle \Delta_0^\dagger \Delta_r \rangle \tag{8}$$

where $\Delta^\dagger$ operator represents creation operator for a singlet pair on neighboring sites:

$$\Delta_i^\dagger = \frac{1}{\sqrt{2}} (c_{i,\downarrow}^\dagger c_{i+1,\uparrow}^\dagger - c_{i,\uparrow}^\dagger c_{i+1,\downarrow}^\dagger) \tag{9}$$

In Fig.4 we compare the long distance behavior of these correlations for various J values, and we find no indication of dominant pairing, in agreement with the previous considerations. Therefore, we are led to conclude that the $\Delta N = 2$ regime is due to a mismatch between the spin and charge velocities. As we will discuss below,
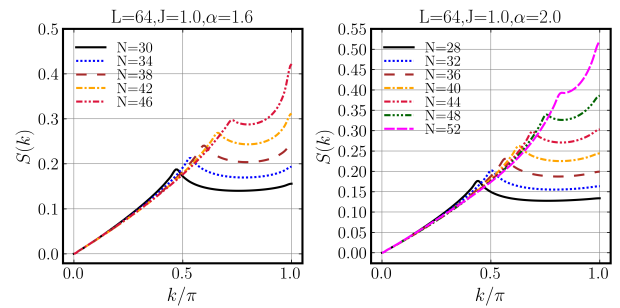

FIG. 7. Spin-spin correlation in momentum space for $J = 1$ and (a) $\alpha = 1.6$ and (b) $\alpha = 2$ and several densities.

for decreasing α holons and spinons will bind into composite quasi-particles, leading the $\Delta N = 2$ window to completely disappear. According to these observations, we deduce that long range antiferromagnetic interactions tend to destroy pairing in favor of phase separation, even at low densities.

We finally comment on the small steps appearing at densities $n \sim 1$ in Fig.1. The first step from the top shows that the single hole configuration is energetically robust. This is a singular case, since it is a $1/L$ effect and speaking of phase separation with only one hole has no significance. However, in open chains we find that the first few holes may tend to cluster at the edges of the chains.

III. QUASI-PARTICLE REGIME

As a consequence of the attraction between spinons and holons, it is possible to realize composite fermionic states that propagate coherently and carry both spin and charge degrees of freedom. These states have been referred to in the literature as "polarons", "mesons" or "string states" (see *e.g.* Ref.65 for a discussion). In this work we favor the idea of a composite state in which spinon and holon "orbit" each other as in a Rydberg-like atom or diatomic molecule where the potential that holds them together, or glue, is a consequence of the long range antiferromagnetic interactions. The argument in favor of quasi-particle formation is more easily understood when presented in the limit of Ising-like interactions in the $t - J_z$ model[104–114]: as a hole is created in the antiferromagnetic background, it does so accompanied by a domain wall, a spinon (see Fig.5). A contact-like local potential proportional to J tends to bind them, but is easily overcome by the kinetic energy of the hole. However, in the presence of RKKY interactions, the effective binding potential is non-local and grows sub-linearly with the separation distance r between hole and spinon due to the string of unaligned spins left behind, as shown in Fig.5(c):

$$V(r) = E_{Ising}(r) - E_{Ising}(r = 1), \tag{10}$$

$$E_{Ising}(r) = \sum_{i \neq j} (-1)^{i-j+1} \frac{\langle 0, r | S_i^z S_j^z | 0, r \rangle}{|i-j|^\alpha}, \qquad (11)$$

where the state $|i, j\rangle$ represents a holon at position i and a spinon at position j. In Fig. 6(c) we show the profile of this potential for different values of α obtained in the Ising limit. Due to the long-range nature of the interactions, the corresponding energy cost would grow with the number of anti-aligned spins. As a result, holon and spinon will now energetically prefer to stick together as a composite object.

In the fully $SU(2)$ spin rotational case, we can numerically calculate the binding energy Δ_b between holon and spinon following a prescription proposed in Ref.[109, 110]. This quantity can be obtained as:

$$\begin{aligned}
\Delta(L) &= E_p(L) - E_s(L) - E_h(L) \qquad (12) \\
&= [E(L, L, 0) + E(L, L-1, 1/2)] \\
&\quad - \frac{1}{2}[E(L-1, L-1, 1/2) + E(L+1, L+1, 1/2)] \\
&\quad - \frac{1}{2}[E(L-1, L-2, 0) + E(L+1, L, 0)]
\end{aligned}$$

where $E(L, N, S^z)$ represents the ground state energy of a system with length L, particle number N and total spin S^z, and L is taken to be even in this definition. The spinon energy E_s is determined by the average ground state of chains with $L \pm 1$ sites at half-filling; the holon energy E_h is obtained by adding one hole; finally, the spinon-holon quasi-particle energy E_p is given by the ground state of chains with L sites at half filling with and without one hole. In these calculations we used periodic boundary conditions with 1600 DMRG states to keep the truncation error under 10^{-6} for system sizes up to $L = 44$. In order to obtain a better extrapolation to the thermodynamic limit we divided the calculation into two groups using (i) $L = 4m$ and $L = 4m - 1$ (ii) $L = 4m + 2$ and $L = 4m + 1$, with $m \in \mathbb{Z}$. To make the extrapolation better conditioned, we flip the sign of hopping term to transfer the lowest energy from $k = \pi$ to $k = 0$ for the chains with length $4m+1$ and one hole(see Ref.109 for details). The extrapolated results as a function of α are shown in panel (a) of Fig. 6. When α is increased through the antiferromagnetic transition into the spin-liquid phase, the binding energy vanishes. We also notice that the data for both $L = 4m$ and $L = 4m+2$ have consistent extrapolations, so we only include the results for $L = 4m + 2$ sector in panel (b) of Fig. 6, which shows the dependence with J for different values of α. Our results indicate a dramatic increase (practically exponential) of the binding energy upon entering into the antiferromagnetically ordered phase.

Notice that similar arguments can be used to explain pairing near half-filling, since the same confining potential would also act between two holes. However, in the presence of RKKY interactions this potential is so strong that it forces the holes to clump together and the system to phase separate, as observed to occur in the phase diagram near half-filling.
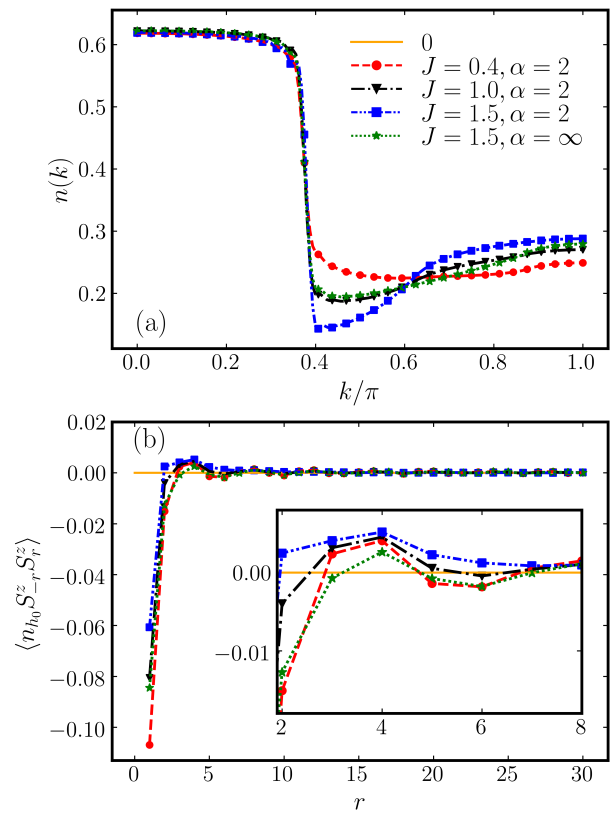

FIG. 8. (a): Momentum distribution function (b): Spin-spin correlations across the hole as defined in the text. The inset shows an enlarged part of the main figure. Results are for a chain of length $L = 64$, density $n = 0.75$, and parameters in the legend.

When the system is deep in the metallic phase, a spin density wave instability appears as a cusp at $k = 2k_F$ in the spin correlations in momentum space:

$$S(k) = \frac{1}{L} \sum_{i,j} e^{ik(i-j)} \langle S_i^z S_j^z \rangle. \qquad (13)$$

In Fig.7 we show the spin structure factor for several values of J and total density $n = N/L$. One can see that as the density increases, a dominant peak appears at $k = \pi$, induced by the RKKY exchange term. The boundary between the low density metallic phase and the high density regime with antiferromagnetic spin correlations is demarked by a dot-dashed line in Figs.2(b) and (c). As observed here, this double-peak structure is not related to phase separation. We postulate that in this window of the phase diagram labeled as "QP", fermionic composite quasi-particles are stable, and that the AFM order survives *inside* the quasi-particles, which can have a large characteristic "size".

As the density is lowered and we enter into the metallic phase, antiferromagnetic correlations are still dominant and the composite quasi-particles persist for a small range of parameters before spinon and holon finally de-

FIG. 9. Photoemission spectrum at half-filling $n = 1$ for $J = 1$ and different values of α ($\alpha = \infty$ indicates the conventional $t-J$ model). The lower panels display cuts in frequency along the $k = \pi/2$ line showing the development of a coherent quasi-particle peak.

confine. We offer two indirect indications that this is the case. The first evidence of fermionic composite states comes from the momentum distribution function $n(k)$, that displays a kink around $k = k_F$ right after crossing the boundary in the phase diagram, as seen in Fig.8(a). This implies the possibility of a jump or discontinuity, instead of a singularity, a sign of finite quasi-particle weight (unfortunately numerical uncertainty makes the calculation of this quantity very unreliable). We also define the correlations across the hole[58, 75] as $\langle n_{h,0} S^z_{-r} S^z_r \rangle$, where the hole is projected on the reference site 0 which is taken to be at the center of the chain. The results shown in Fig.8(b) are normalized by $\langle n_{h,0} \rangle$. In the quasi-particle regime we find that spins equidistant from the

hole are aligned in the same direction. This is consistent with a charge and spin configuration as the one depicted in Fig.5(a), corresponding to a composite state of a spinon and a holon. Notice that the correlations at distance $r = 1$ in Fig.8(b) are antiferromagnetic, indicating fluctuations with a heavy contribution from the configurations in Fig.5(b), that is to be expected since the quasi-particle moves combining hopping and spin-flip processes. Outside of the quasi-particle regime, the correlations across the hole tend to oscillate with momentum $2k_F$ indicating deconfined spinons and holons, as illustrated in Fig.5(c). The presence of coherent quasi-particles will be supported by calculations of the photoemission spectra in the following section.

IV. SINGLE HOLE SPECTRAL FUNCTION

A. DMRG at half-filling

We are seeking signatures of coherent quasi-particles in the photoemission spectrum of the generalized $t - J$

model with long-range RKKY interactions using the time-dependent DMRG method (tDMRG) [115–118].
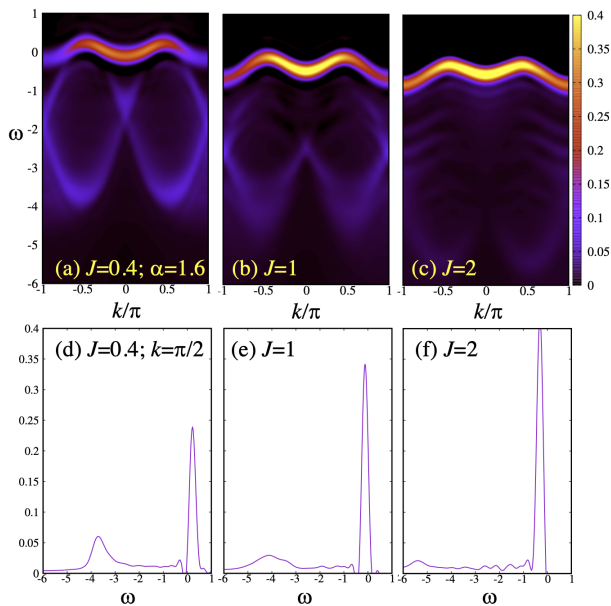
FIG. 10. Top row: Photoemission spectrum at half-filling $n = 1$ for $\alpha = 1.6$, deep into the Néel phase and different values of J. Bottom row: cuts in frequency along the $k = \pi/2$ line showing the development of a coherent quasi-particle band splitting from the continuum.

We follow the standard prescription detailed in the original work Ref.[115] and subsequent studies of the Hubbard model[119, 120]. We calculate the two-time correlator:

$$\langle c_{r\uparrow}^{\dagger}(t)c_{0\uparrow}(0)\rangle = \langle \psi_0| e^{iHt} c_{r\uparrow}^{\dagger} e^{-iHt} c_{0\uparrow}|\psi_0\rangle, \qquad (14)$$

where $c_{0\sigma}$ here is defined at the center of the chain, and r is the distance from center. By Fourier transforming to momentum and frequency, we reconstruct the momentum resolved spectral function. This procedure is carried out numerically over a finite time window t_{max} with $t_{max} = 20$ unless otherwise stated. In order to attenuate artificial ringing we use standard windowing techniques. The spectrum will exhibit an artificial broadening that is inversely proportional to t_{max}. The long-range terms in the Hamiltonian make it convenient to use a time-step targeting procedure with a Krylov expansion of the time-evolution operator [121] and a time step $\delta t = 0.1$ (time is measured in units of hopping t^{-1} and t is our unit of energy). We study chains of length $L = 48$ using up to 400 DMRG states that guarantees that the truncation error remains smaller than 10^{-6} over the time window. In all results shown here we introduced a shift in ω given by $\mu = E_1 - E_0$, where E_0 is the energy of the ground state $|\psi_0\rangle$ with $N = L$ and $E_1 = \langle \psi_1|H|\psi_1\rangle / \langle \psi_1|\psi_1\rangle$ with $|\psi_1\rangle = c_{L/2}|\psi_0\rangle$.

We show results at half-filling in Fig.9 for $J/t = 1$ and varying α across the transition from Néel to spin liquid. The spectral function of the conventional $t - J$ is displayed in panel Fig.9(d). The spectrum displays features of both spinon and holon dispersions[122, 123]: assum-
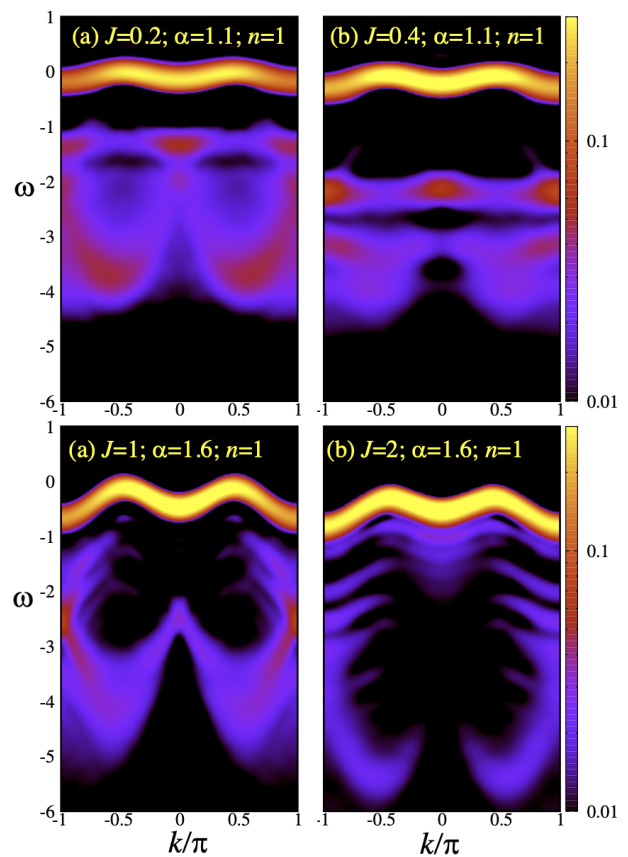

FIG. 11. Photoemission spectrum for a single hole for several values of J and α in a color log scale, showing features associated with strings inside the continuum.

ing holon and spinons dispersions $\epsilon_h(q_h)$ and $\epsilon_s(q_s)$, one can construct all possible energies with momentum k as $\epsilon(k) = \epsilon_h(q_h) + \epsilon_s(q_s)$, with $k = q_h + q_s$. Clearly, this construction will yield a continuum of energies with momentum k. The figures show the development of a coherent quasi-particle peak as we cross the critical value of $\alpha_c \sim 2.2$ from above. In addition, we observe that the dispersion develops two minima. This is explained by realizing that the composite quasi-particles will have to move by means of a combination of hopping and spin flips. Therefore, the particle will effectively acquire a second (next-nearest) neighbor hopping contribution since each spin flip moves a spinon by two sites. In the lower panels of the same figure we show cuts along the $k = k_F = \pi/2$ line. We can clearly resolve the quasi-particle peak splitting from the upper edge of the continuum (ringing oscillations are artifacts of the Fourier transform, as noted above).

In Fig.10 we compare the behavior with varying J at a fixed value of $\alpha = 1.6$, deep into the AFM ordered phase, where we see an increase of spectral weight in the quasi-particle band with increasing J. Looking more carefully, we notice the development of new structures inside the incoherent continuum. In order to resolve these
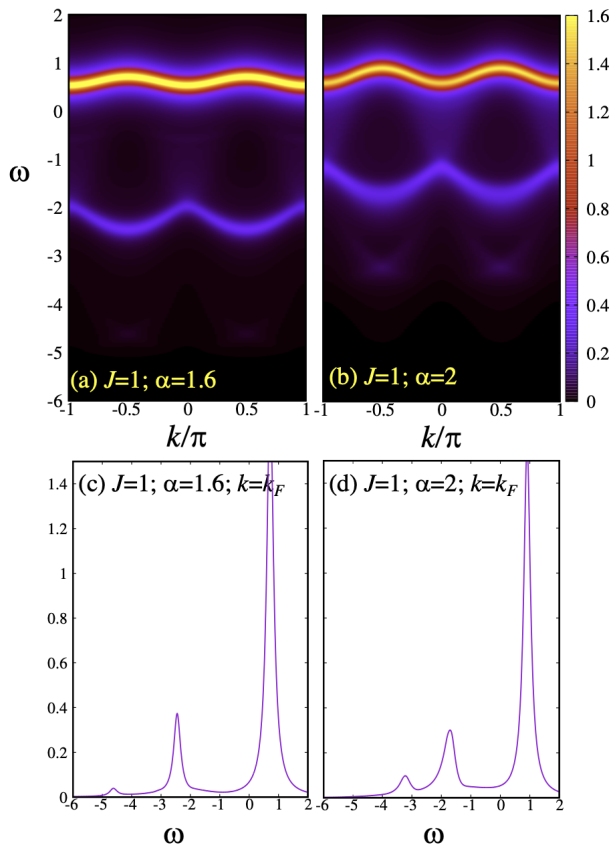
FIG. 12. Photoemission spectrum at half-filling $n = 1$ for $J = 1$ and different values of α obtained with the self-consistent Born approximation (SCBA). In the lower panels (c) and (d) We show cuts in frequency along the $k = \pi/2$ line.

new features, we plot the spectral weight in a log scale in Fig.11. The "ladder" appearing inside the continuum is not a numerical artifact but a manifestation of the string confining potential (10). These "string" excitations are not stable, and decay into a spinon and a holon as we discuss below. We also look at two extreme cases with $\alpha = 1.1$ and small $J = 0.2$ and 0.4 in panels (a) and (b) of the same figure, where we observe just one or two prominent string states. One way to interpret the energy spacing between them is by considering a simplistic picture in which spinons cannot move and holes behave as particles trapped by the confining potential of Fig.6. In a linear potential, these bound states would be Airy functions with equally spaced energy levels [106]. In our case, the behavior is less trivial, but analogous, with a spacing that increases with increasing J or with smaller α. We provide a more detailed theoretical description and analysis in the following sections.

B. SCBA

In order to gain further physical insight, we compare the DMRG photoemission spectra with the predictions

of an analytic approach that correctly describes the motion of a hole tightly coupled with the semiclassical spin-wave excitations of an antiferromagnetic state, giving rise to a spin-polaron quasiparticle. Hence, we have calculated the single hole spectral functions by means of the self-consistent Born approximation (SCBA) [124–127], a method that has been proven to compare quantitatively very well with exact diagonalization (ED) results on finite two-dimensional clusters with short range interactions in different antiferromagnets [124, 128–131]. It is one of the more reliable and checked analytical methods up to date to calculate the hole Green's function, and in particular, its QP dispersion relation. In order to do such calculation, we follow standard procedures [124]. On one hand, the magnetic elementary excitations are obtained treating the Heisenberg exchange terms of the Hamiltonian at the linear spin-wave (LSW) approximation. Thus, we restrict this description to the long range magnetically ordered regime of the phase diagram, whose magnetic spectrum consists of semiclassical magnons within the LSW approximation. In this sense, the SCBA will have the ability to exhibit the physics of a single hole interacting with one-dimensional magnons only, excluding other possible excitations like spinons. On the other hand, the electron creation and annihilation operators in the hopping terms are mapped into holons in the slave-fermion representation (details in the Supplementary Material of Ref. [132]). Within SCBA, we arrive at an effective Hamiltonian:

$$H_{\text{eff}} = \sum_{\mathbf{k}} \omega_{\mathbf{k}} \theta_{\mathbf{k}}^{\dagger} \theta_{\mathbf{k}} + \frac{2S}{\sqrt{N}} \sum_{\mathbf{kq}} \left(M_{\mathbf{kq}} h_{\mathbf{k}}^{\dagger} h_{\mathbf{k-q}} \theta_{\mathbf{q}} + \text{H.c.} \right),$$
(15)

where there is no hole tight-binding-like free hopping term, since the ground state magnetic pattern consists in a 180° antiferromagnetic Néel order. The magnon dispersion relation $\omega_{\mathbf{k}}$ is given by [93, 94]:

$$\omega_{\mathbf{k}} = \sqrt{\varepsilon_{\mathbf{k}}^2 - g_{\mathbf{k}}^2},$$
(16)

$$\varepsilon_{\mathbf{k}} = 2JS \sum_{n=1}^{L/2} \frac{1}{(2n-1)^{\alpha}} - 2JS \sum_{n=1}^{L/2} \frac{\cos(2nk) - 1}{(2n)^{\alpha}}$$

$$g_{\mathbf{k}} = -2JS \sum_{n=1}^{L/2} \frac{\cos[(2n-1)k]}{|2n-1|^{\alpha}},$$
(17)

and $M_{\mathbf{kq}}$ is the vertex interaction that couples the hole with magnons:

$$M_{\mathbf{kq}} = 2t[\cos(k)u_{k-q} + \cos(q)v_{k-q}],$$
(18)

where u_k and v_k are the usual Bogoliubov coefficients. We have evaluated the sums in (17) up to where convergence is reached within a given tolerance. The self energy is calculated within the SCBA taking into account non-crossing diagrams only, which leads to the self consistent

equation

$$\Sigma_k(\omega) = \frac{1}{L} \sum_q \frac{|M_{kq}|^2}{\omega + i\epsilon - \omega_{k-q} - \Sigma_q(\omega - \omega_{k-q})} \quad (19)$$

from which the hole spectral function is obtained.

In Fig. 12 the SCBA spectrum is shown. All the SCBA results are for $L = 100$ sites, as it was checked that it already accurately describes the thermodynamic limit. Similar to the DMRG results, Fig. 10, the SCBA spectrum also shows a well defined quasiparticle band and a high energy continuum. However, in this case, the high energy spectrum is clearly composed of strings. Strings are well known manifestations of chains of misaligned spins left behind by the hole as it hops [124, 125]. As previously discussed, as the hole hops, misaligned spins are left behind, creating an energy potential that binds the hole, promoting its return to the original position. As in 1D there are no closed Trugman loops [133], the only option for the hole to "cure" the strings of wrongly aligned spins is to retrace its path. In this picture, the energy cost of moving the hole increases with distance, such that it is favorable for the hole to return to its original position by reabsorbing the magnetic excitations, in this case magnons, in reverse order of creation. These processes produce non-crossing diagrams that are precisely what lies underneath the SCBA. However, the presence of spin-flip interactions in the Hamiltonian offers an alternative channel for the magnetic fluctuations to repair the misaligned spins, giving the hole the possibility of moving coherently. These processes are responsible for the QP peak in the spectrum. In the case of the $t - J_z$ Ising case, it has been shown that the (k-independent) spectrum consists of several strings [111]. In our model the same physics appears when $\alpha \simeq 1$, as the magnetic order becomes almost classical, with a very low probability of spin-flip processes. As α increases and the long range order is weakened, the QP spectral weight decreases, and the high energy string continuum gains weight, but the SCBA picture remains essentially the same.

In Fig. 13 we show the SCBA spectra at low α, where the order is more rigid, varying J/t. At low J/t, where the characteristic time of magnetic fluctuations is much larger than that of the hole hopping, strings are manifested.

On one hand, the QP spectrum of the SCBA and DMRG show good qualitative agreement in the ordered regime of the phase diagram, i.e. for $\alpha < 2.2$. This indicates that the QP in the ordered regime is effectively a magnetic polaron, where the hole dynamics is determined by its interaction with magnons. However, the high energy spectrum of the SCBA and DMRG differ, especially when J/t and α are not very low. For low α both methods show a string picture. However, strings are unstable at high energies and decay into a continuum of spinon-holon excitations. On the other hand, in the SCBA approximation, strings spread over the entire energy range and are mostly responsible for the incoherent
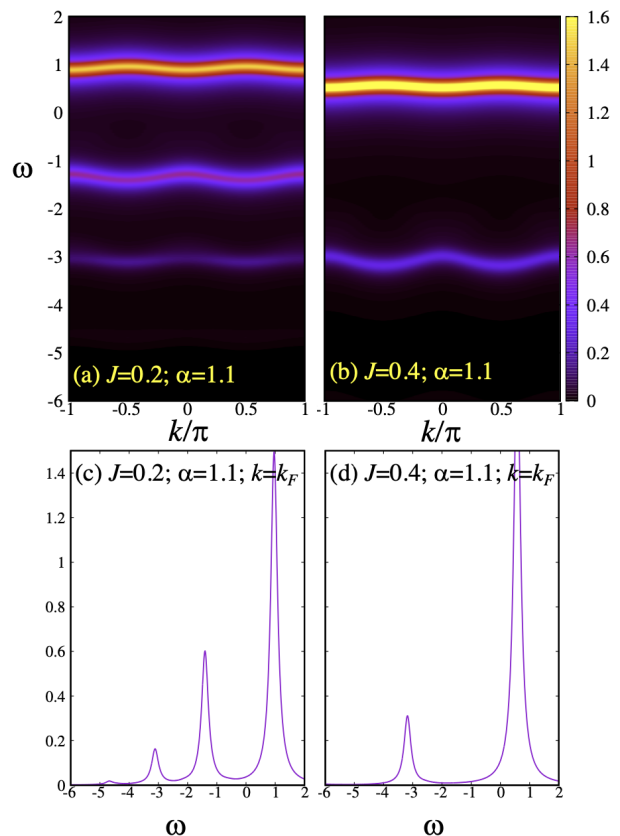

FIG. 13. Photoemission spectrum at half-filling $n = 1$ for $\alpha = 1.1$ and different values of J obtained with the self-consistent Born approximation (SCBA). In the lower panels (c) and (d) We show cuts in frequency along the $k = \pi/2$ line.

part of the spectrum. The noticeable differences between both methods in the intermediate to high energy sector arise because in the SCBA, due to the linear spin wave treatment of the magnetic spectrum, spinons are absent, and spin-charge separation is not possible.

Hence, it can be concluded that the exact DMRG spectrum exhibits a spin-polaron quasiparticle at the lowest energy, and a few unstable strings for low α, a typical behavior in higher dimension antiferromagnets. This QP is the result of the confinement of the holon and spinon excitations at low energies, while for higher energies there are signatures of spin-charge separation even for $\alpha < 2.2$, where there is long range order. Hence, the 1D RKKY system displays signatures of a dimensional crossover as a function of the energy, with the 1D physics surviving at high energies.

C. Spinon-holon problem

In order to provide an intuitive physical picture that accounts for spin charge separation and can allow us to peek into the internal structure of the composite quasiparticle, we start from the Ising limit, in which the
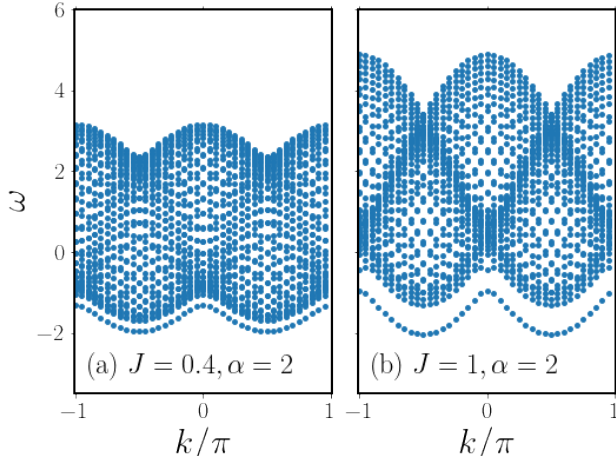
translationally invariant and labeled by a momentum k:

$$|r, k\rangle = \frac{1}{\sqrt{L}} \sum_{x=0}^{L-1} e^{ikx} T_x |r_s = 0, r_h = r\rangle. \quad (21)$$

$$= \frac{1}{\sqrt{L}} \sum_{x=0}^{L-1} e^{ikx} |r_s = x, r_h = r + x\rangle$$

In this basis, the Hamiltonian matrix can be easily obtained and numerically diagonalized for each momentum sector. The spectrum of a chain with $L = 40$ sites is shown in Fig.14 for $\alpha = 2$, $J = 0.4$ and 1. Without interactions, the spectrum consists of a continuum with a lower edge given by $\omega(k) = \epsilon_s(k) - \epsilon_h(k = 0) = \epsilon_s(k) - 2$. Long-range interactions favor the formation of composite fermionic bound states splitting from the spinon-holon continuum, resembling our numerical results obtained with DMRG and the SCBA in previous sections. However, in this picture the spinon-holon continuum is manifest while the SCBA cannot account for it. Despite being a crude approximation, it offers intuition about the nature of the quasi-particle excitations: the hole and spinon form a Rydberg-like state or diatomic molecule, confined by the string potential of Fig.6. In order to move coherently, the spinon-holon pair has to do it in two steps: first, a spin flip moves the spinon by two sites; second, the holon needs to follow and settle in between the two parallel spins. As a consequence, the dispersion of the "polaron" will display two minima, as already observed, with a bandwidth determined primarily by J.

V. PHOTOEMISSION AT FINITE DOPING

At finite doping the existence of coherent quasiparticles in one-dimension is less expected. One argument against it is the presence of pervasive nesting at all densities, making Fermi liquid theory unstable and LL theory apparently unavoidable. However, in Fig. 15 we show the spectrum at momentum $k = k_F$ at density $n = 0.75$ for the conventional $t - J$ model displaying a Fermi edge singularity, and $\alpha = 2$, showing a coherent peak that seems to split from the continuum. This numerical evidence suggests that indeed quasiparticles may be stable, at least in a range of (relatively high) densities. We postulate, without offering a proof, that this occurs whenever the spin correlations have a dominant AFM peak at $k = \pi$, the region labeled as "QP" in Fig.2.

VI. CONCLUSIONS

We have studied the stability of fermionic quasiparticles in a doped antiferromagnet in a relatively simple one-dimensional model that realizes much of the phenomenology of the higher dimensional $t - J$ model. At half-filling, the all-to-all-interactions lead to a transition to a phase with spontaneous symmetry breaking and Néel

FIG. 14. Spectrum of the spinon-holon problem for two different values of J and $\alpha = 2$.

ground state without a hole is just a trivial classical Néel order. When the insulator is doped with a hole it introduces a domain wall (a spinon) in the AFM background, as shown in Fig.5(a). Besides the motion of the hole, we consider additional quantum fluctuations mediated by spin-flip processes that allow the domain wall to move, ignoring processes that create new spinons for being energetically too costly (this includes long-range spin-flips).

In order to make this scenario more concrete, we explicitly solve the two-body problem of a spinon and a holon. As noted previously, the spinon propagates by *two* sites with each spin-flip, and therefore it has a dispersion $\epsilon_s(k) = J\cos(2k)$, while the holon dispersion is $\epsilon_h(k) = -2t\cos(k)$. Both particles interact via a confining potential $V(r)$, Eq.10), where r is the separation between the two. The formulation we use to study the two particle bound state has been extensively applied in a number of scenarios in the literature, including Hubbard-like models[134–140], the formation of excitons in multi-band problems[141], and magnons [98]. In our case, as the hole and spinon move apart, they leave behind a string of anti-aligned spins in the antiferromagnetic background that, unlike the conventional 1D $t-J$ model, costs an energy that grows with the relative distance between spinon and holon – the length of the string. In our case, we assume the following Hamiltonian:

$$H|r_s, r_h\rangle = -t(|r_s, r_h + 1\rangle + |r_s, r_h - 1\rangle) \\ + J/2(|r_s + 2, r_h\rangle + |r_s - 2, r_h\rangle). \\ + V(|r_s - r_h|)|r_s, r_h\rangle, \quad (20)$$

where r_s and r_h refer to the position of the spinon and holon respectively, and the potential V is given by Eq. (10). We consider periodic boundary conditions, which allows us to construct a basis of states that are
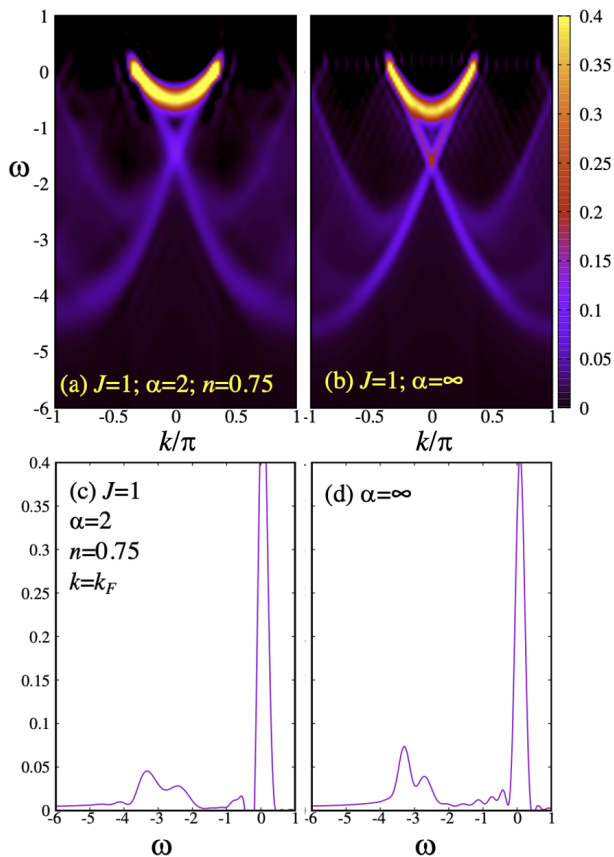
FIG. 15. Photoemission spectrum at density $n = 0.75$ for $J = 1$, $\alpha = 1.6$ and the conventional $t - J$ model ($\alpha = \infty$). We show cuts in frequency along the $k = k_F$ line showing the development of a coherent quasi-particle peak.

order. Interestingly, pairing is no longer stable and gets replaced by a large region where phase separation into AFM and hole-rich domains takes place: long-range interactions lead to holes clumping, or clustering, indicating that in order to stabilize and have mobile pairs, a weaker confining potential might be required. Such scenarios have been explored in the conventional $t-J$ model with a staggered magnetic field where the potential is linear and pairing is robust[106], or in a square lattice with long range AFM order but where the holes are allowed to move only along the x direction [63]. In the context of our model, one possible way to counteract the instability toward phase separation is by including a long range Coulomb repulsion and second-neighbor hopping to increase the hole kinetic energy. Work in this direction is underway.

Upon doping the antiferromagnet with a hole, we observe spinons and holons binding to form composite quasiparticles in the regime with long-range antiferromagnetism for small α, while they remain deconfined in the spin-liquid phase for $\alpha > \alpha_c \sim 2.2$. These excitations appear in the photoemission spectrum in the form of a coherent band splitting from the edge of the con-

tinuum of width determined by the exchange J and the exponent α. This band has also been observed in calculations on the 2D Hubbard model[15, 25, 26, 142, 143] and $t - J$ model [65]. The composite nature of the quasi-particles is supported by calculations of the spinon-holon binding energy that show a dramatic enhancement upon transitioning to the Néel phase and it is analogous to the observed physics in doped two dimensional antiferromagnets[124, 130, 144]. This picture is further confirmed by SCBA calculations and the spectra of the spinon-holon problem. While the system exhibits well defined fermionic quasi-particles, their internal structure can be described as a spinon and holon oscillating around a common center of mass. Also, the SCBA calculations exhibit high energy strings in the long range ordered regime, but this physics is present in the DMRG calculations only at very low α, where the magnetic order is very rigid. This leads us to conclude that a single hole, even in the ordered phase, couples at high energies to magnetic excitations that are spinons instead of magnons.

The physical size of the composite quasi-particle can be quite large, and will be dictated by both J and α and will diverge at the transition point α_c. As a matter of fact, it might be possible that close enough to α_c the size of the "polaron" can be larger than the chain length, in which case one would only see spin-charge separation. At higher energies, both spinon and holon deconfine and we observe a continuum that can be associated with the original dispersions of the two objects. Therefore, while the system exhibits higher-dimensional physics at low energies, the 1D physics of spin-charge separation re-emerges at higher energies. This implies that at finite temperature, larger than the binding energy between holon and spinon, the quasi-particles would decay into their original constituents, establishing a limitation to our experimental ability to resolve them.

At finite doping, upon crossing the phase separated region, we encounter evidence of surviving quasiparticles near the Fermi points. This is a quite puzzling surprise, since one would expect a 1D metal to be a Luttinger Liquid due to nesting and the fact that the Fermi surface consists only of discrete points (we are loosely referring to the regime with spin-charge separation as the LL phase, even though the excitation spectrum is no longer linear in the presence of long-range interactions). In fact, at low densities, the AFM order melts and spin charge separation re-emerges. However, it may seem as though the confining potential is strong enough to induce dominant AFM interactions and coherent quasi-particles even away from half-filling, albeit in a narrow window of densities. We point out that one-dimensional metals with fermionic quasi-particles are indeed possible, but this typically occurs in gapped systems, such as ladders.[145–148] In these systems the spin and charge gap may survive at finite doping[149]. However, our model Eq. (3) is gapless in both channels. Further numerical and theoretical work is needed to elucidate the mechanisms that might possibly stabilize fermionic quasi-particles in this regime.

Finally, this work demonstrates the interesting phenomenology that can arise from the inclusion on long range interactions and, in particular, establishes Eq. (3) as a rich toy model Hamiltonian to study higher dimensional physics with methods usually considered more amenable to one dimensional problems.

VII. ACKNOWLEDGMENTS

[1] E. Dagotto, Correlated electrons in high-temperature superconductors, Rev. Mod. Phys. **66**, 763 (1994).

[2] P. A. Lee, N. Nagaosa, and X.-G. Wen, Doping a mott insulator: Physics of high-temperature superconductivity, Rev. Mod. Phys. **78**, 17 (2006).

[3] M. Imada, A. Fujimori, and Y. Tokura, Metal-insulator transitions, Rev. Mod. Phys. **70**, 1039 (1998).

[4] D. Scalapino, Numerical studies of the 2d hubbard model, in *Handbook of High-Temperature Superconductivity*, edited by J. Schrieffer and J. Brooks (Springer New York, 2007) pp. 495–526.

[5] M. Qin, T. Schäfer, S. Andergassen, P. Corboz, and E. Gull, The hubbard model: A computational perspective (2021), arXiv:2104.00064 [cond-mat.str-el].

[6] J. P. F. LeBlanc, A. E. Antipov, F. Becca, I. W. Bulik, G. K.-L. Chan, C.-M. Chung, Y. Deng, M. Ferrero, T. M. Henderson, C. A. Jiménez-Hoyos, E. Kozik, X.-W. Liu, A. J. Millis, N. V. Prokof'ev, M. Qin, G. E. Scuseria, H. Shi, B. V. Svistunov, L. F. Tocchio, I. S. Tupitsyn, S. R. White, S. Zhang, B.-X. Zheng, Z. Zhu, and E. Gull (Simons Collaboration on the Many-Electron Problem), Solutions of the two-dimensional hubbard model: Benchmarks and results from a wide range of numerical algorithms, Phys. Rev. X **5**, 041041 (2015).

[7] M. Qin, C.-M. Chung, H. Shi, E. Vitali, C. Hubig, U. Schollwöck, S. R. White, and S. Zhang (Simons Collaboration on the Many-Electron Problem), Absence of superconductivity in the pure two-dimensional hubbard model, Phys. Rev. X **10**, 031016 (2020).

[8] H. Frahm and V. E. Korepin, Phys. Rev. B **42**, 10553 (1990).

[9] K. Penc, K. Hallberg, F. Mila, and H. Shiba, Phys. Rev. B **55**, 15475 (1997).

[10] E. Jeckelmann, F. Gebhard, and F. H. L. Essler, Phys. Rev. Lett. **85**, 3910 (2000).

[11] H. Benthien, F. Gebhard, and E. Jeckelmann, Phys. Rev. Lett. **92**, 256401 (2004).

[12] J. M. P. Carmelo, K. Penc, L. M. Martelo, P. D. Sacramento, J. M. B. Lopes Dos Santos, R. Claessen, M. Sing, and U. Schwingenschlögl, Europhys. Lett. **67**, 233 (2004).

[13] J. M. P. Carmelo, K. Penc, P. D. Sacramento, M. Sing, and Claessen, J. Phys. Cond. Mat. **18**, 5191 (2006).

[14] J. M. P. Carmelo, D. Bozi, and K. Penc, J. Phys. Cond. Mat. **20**, 415103 (2008).

[15] M. Kohno, Spectral Properties near the Mott Transition in the One-Dimensional Hubbard Model, Phys. Rev. Lett. **105**, 106402 (2010).

[16] T. L. Schmidt, Imambekov A., and L. I. Glazman, Phys. Rev. Lett. **104**, 116403 (2010).

[17] R. G. Pereira and E. Sela, Phys. Rev. B **82**, 115324 (2010).

[18] F. H. L. Essler, Phys. Rev. B **81**, 205120 (2010).

[19] T. L. Schmidt, A. Imambekov, and L. I. Glazman, Phys. Rev. B **82**, 245104 (2010).

[20] A. Imambekov, T. L. Schmidt, and L. I. Glazman, Rev. Mod. Phys. **84**, 1253 (2012).

[21] L. Seabra, F. H. L. Essler, F. Pollmann, I. Schneider, and T. Veness, Phys. Rev. B **90**, 245127 (2014).

[22] F. H. L. Essler, R. G. Pereira, and I. Schneider, Phys. Rev. B **91**, 245150 (2015).

[23] A. C. Tiegel, T. Veness, P. E. Dargel, A. Honecker, T. Pruschke, I. P. McCulloch, and F. H. L. Essler, Phys. Rev. B **93**, 125108 (2016).

[24] T. Veness and F. H. L. Essler, Phys. Rev. B **93**, 205101 (2016).

[25] C. Yang and A. E. Feiguin, Spectral function of the two-dimensional hubbard model: A density matrix renormalization group plus cluster perturbation theory study, Phys. Rev. B **93**, 081107(R) (2016).

[26] Y. Wang, K. Wohlfeld, B. Moritz, C. J. Jia, M. van Veenendaal, K. Wu, C.-C. Chen, and T. P. Devereaux, Origin of strong dispersion in hubbard insulators, Phys. Rev. B **92**, 075119 (2015).

[27] S.-i. Tomonaga, Remarks on Bloch's Method of Sound Waves applied to Many-Fermion Problems, Progress of Theoretical Physics **5**, 544 (1950), https://academic.oup.com/ptp/article-pdf/5/4/544/5430161/5-4-544.pdf.

[28] J. M. Luttinger, An exactly soluble model of a many-fermion system, Journal of Mathematical Physics **4**, 1154 (1963).

[29] D. C. Mattis and E. H. Lieb, Exact solution of a many-fermion system and its associated boson field, Journal of Mathematical Physics **6**, 304–312 (1965).

[30] F. D. M. Haldane, 'luttinger liquid theory' of one-dimensional quantum fluids. i. properties of the luttinger model and their extension to the general 1d interacting spinless fermi gas, Journal of Physics C: Solid State Physics **14**, 2585 (1981).

[31] A. O. Gogolin, A. A. Nerseyan, and A. M. Tsvelik, *Bosonization and Strongly Correlated Systems* (Cambridge University Press, Cambridge, England, 1998).

[32] T. Giamarchi, *Quantum Physics in One Dimension* (Clarendon Press, Oxford, 2004).

[33] F. H. L. Essler and A. M. Tsvelik, Finite temperature spectral function of mott insulators and charge density wave states, Phys. Rev. Lett. **90**, 126401 (2003).

[34] J. M. P. Carmelo, T. Čadež, and P. D. Sacramento, One-particle spectral functions of the one-dimensional fermionic hubbard model with one fermion per site at zero and finite magnetic fields, Phys. Rev. B **103**, 195129 (2021).

[35] E. H. Lieb and F. Y. Wu, Absence of mott transition in an exact solution of the short-range, one-band model in one dimension, Phys. Rev. Lett. **20**, 1445 (1968).

[36] E. H. Lieb and F. Wu, The one-dimensional hubbard model: a reminiscence, Physica A: Statistical Mechanics and its Applications **321**, 1 (2003), statphys-Taiwan-2002: Lattice Models and Complex Systems.

[37] F. Essler, H. Frahm, F. Göhmann, A. Klümper, and V. E. Korepin, *The One-Dimensional Hubbard Model* (Cambridge University Press, Cambridge, England, 2010).

[38] P. A. Bares and G. Blatter, Supersymmetric t-j model in one dimension: Separation of spin and charge, Phys. Rev. Lett. **64**, 2567 (1990).

[39] P.-A. Bares, G. Blatter, and M. Ogata, Exact solution of the t-j model in one dimension at $2t=\pm j$: Ground state and excitation spectrum, Phys. Rev. B **44**, 130 (1991).

[40] S. Sarkar, J. Phys. A: Math. Gen. **24**, 1137 (1991).

[41] F. H. L. Essler and V. E. Korepin, Higher conservation laws and algebraic bethe ansätze for the supersymmetric t-j model, Phys. Rev. B **46**, 9147 (1992).

[42] A. Moreno, A. Muramatsu, and J. M. P. Carmelo, Charge and spin fractionalization beyond the luttinger-liquid paradigm, Phys. Rev. B **87**, 075101 (2013).

[43] N. D. Mermin and H. Wagner, Absence of ferromagnetism or antiferromagnetism in one- or two-dimensional isotropic heisenberg models, Phys. Rev. Lett. **17**, 1133 (1966).

[44] B. I. Halperin, On the hohenberg–mermin–wagner theorem and its limitations, Journal of Statistical Physics **175**, 521 (2019).

[45] M. E. Zhitomirsky and A. L. Chernyshev, Colloquium: Spontaneous magnon decays, Rev. Mod. Phys. **85**, 219 (2013).

[46] W. O. Putikka, R. L. Glenister, R. R. P. Singh, and H. Tsunetsugu, Indications of spin-charge separation in the two-dimensional t-j model, Phys. Rev. Lett. **73**, 170 (1994).

[47] Y. C. Chen, A. Moreo, F. Ortolani, E. Dagotto, and T. K. Lee, Spin-charge separation in the two-dimensional hubbard and t-j models at low electronic density, Phys. Rev. B **50**, 655 (1994).

[48] S. Haas and E. Dagotto, Photoemission spectra in $t-j$ ladders with two legs, Phys. Rev. B **54**, R3718 (1996).

[49] T. M. Rice, S. Haas, M. Sigrist, and F.-C. Zhang, Lightly doped $t-j$ three-leg ladders: An analog for the underdoped cuprates, Phys. Rev. B **56**, 14655 (1997).

[50] G. B. Martins, R. Eder, and E. Dagotto, Indications of spin-charge separation in the two-dimensional extended t-j model, Phys. Rev. B **60**, R3716 (1999).

[51] D. Boies, C. Bourbonnais, and A. M. S. Tremblay, One-particle and two-particle instability of coupled luttinger liquids, Phys. Rev. Lett. **74**, 968 (1995).

[52] D. Poilblanc, D. J. Scalapino, and W. Hanke, Spin and charge modes of the t-J ladder, Phys. Rev. B **52**, 6796 (1995).

[53] E. Arrigoni, Crossover from luttinger- to fermi-liquid behavior in strongly anisotropic systems in large dimensions, Phys. Rev. Lett. **83**, 128 (1999).

[54] A. Vishwanath and D. Carpentier, Two-dimensional anisotropic non-fermi-liquid phase of coupled luttinger liquids, Phys. Rev. Lett. **86**, 676 (2001).

[55] P. W. Anderson, Spin-charge separation is the key to the high Tc cuprates, Phys. C Supercond. **341-348**, 9 (2000).

[56] M. Brunner, S. Capponi, F. F. Assaad, and A. Muramatsu, Single hole dynamics in the t-j model on two- and three-leg ladders, Phys. Rev. B **63**, 180511(R) (2001).

[57] G. B. Martins, C. Gazza, J. C. Xavier, A. Feiguin, and E. Dagotto, Doped stripes in models for the cuprates emerging from the one-hole properties of the insulator, Phys. Rev. Lett. **84**, 5844 (2000).

[58] G. B. Martins, J. C. Xavier, C. Gazza, M. Vojta, and E. Dagotto, Indications of spin-charge separation at short distance and stripe formation in the extended t-j model on ladders and planes, Phys. Rev. B **63**, 014414 (2000).

[59] A. S. Mishchenko, N. V. Prokof'ev, and B. V. Svistunov, Single-hole spectral function and spin-charge separation in the $t-j$ model, Phys. Rev. B **64**, 033101 (2001).

[60] A. Läuchli and D. Poilblanc, Spin-charge separation in two-dimensional frustrated quantum magnets, Phys. Rev. Lett. **92**, 236404 (2004).

[61] J. Bonča, S. Maekawa, and T. Tohyama, Numerical approach to the low-doping regime of the $t-j$ model, Phys. Rev. B **76**, 035121 (2007).

[62] B. Moritz, F. Schmitt, W. Meevasana, S. Johnston, E. M. Motoyama, M. Greven, D. H. Lu, C. Kim, R. T. Scalettar, Z.-X. Shen, and T. P. Devereaux, Effect of strong correlations on the high energy anomaly in hole- and electron-doped high-tcsuperconductors, New J. Phys. **11**, 093020 (2009).

[63] F. Grusdt, Z. Zhu, T. Shi, and E. Demler, Meson formation in mixed-dimensional t-J models, SciPost Phys. **5**, 57 (2018).

[64] F. Grusdt, A. Bohrdt, and E. Demler, Microscopic spinon-chargon theory of magnetic polarons in the $t-j$ model, Phys. Rev. B **99**, 224422 (2019).

[65] A. Bohrdt, E. Demler, F. Pollmann, M. Knap, and F. Grusdt, Parton theory of angle-resolved photoemission spectroscopy spectra in antiferromagnetic mott insulators, Phys. Rev. B **102**, 035139 (2020).

[66] R. Jordens, N. Strohmaier, K. Gunter, H. Moritz, and T. Esslinger, A mott insulator of fermionic atoms in an optical lattice, Nature **455**, 204 (2008).

[67] T. Esslinger, Fermi-hubbard physics with atoms in an optical lattice, Annual Review of Condensed Matter Physics **1**, 129 (2010), https://doi.org/10.1146/annurev-conmatphys-070909-104059.

[68] M. Endres, M. Cheneau, T. Fukuhara, C. Weitenberg, P. Schauß, C. Gross, L. Mazza, M. C. Bañuls, L. Pollet, I. Bloch, and S. Kuhr, Observation of correlated particle-hole pairs and string order in low-

dimensional mott insulators, Science **334**, 200 (2011), http://science.sciencemag.org/content/334/6053/200.full.pdf.

[69] I. M. Georgescu, S. Ashhab, and F. Nori, Quantum simulation, Rev. Mod. Phys. **86**, 153 (2014).

[70] R. A. Hart, P. M. Duarte, T.-L. Yang, X. Liu, T. Paiva, E. Khatami, R. T. Scalettar, N. Trivedi, D. A. Huse, and R. G. Hulet, Observation of antiferromagnetic correlations in the hubbard model with ultracold atoms, Nature **519**, 211 EP (2015).

[71] P. M. Duarte, R. A. Hart, T.-L. Yang, X. Liu, T. Paiva, E. Khatami, R. T. Scalettar, N. Trivedi, and R. G. Hulet, Compressibility of a fermionic mott insulator of ultracold atoms, Phys. Rev. Lett. **114**, 070403 (2015).

[72] M. Boll, T. A. Hilker, G. Salomon, A. Omran, J. Nespolo, L. Pollet, I. Bloch, and C. Gross, Spin- and density-resolved microscopy of antiferromagnetic correlations in fermi-hubbard chains, Science **353**, 1257 (2016), http://science.sciencemag.org/content/353/6305/1257.full.pdf.

[73] L. W. Cheuk, M. A. Nichols, K. R. Lawrence, M. Okan, H. Zhang, E. Khatami, N. Trivedi, T. Paiva, M. Rigol, and M. W. Zwierlein, Observation of spatial charge and spin correlations in the 2d fermi-hubbard model, Science **353**, 1260 (2016), http://science.sciencemag.org/content/353/6305/1260.full.pdf.

[74] P. T. Brown, D. Mitra, E. Guardado-Sanchez, P. Schauß, S. S. Kondov, E. Khatami, T. Paiva, N. Trivedi, D. A. Huse, and W. S. Bakr, Spin-imbalance in a 2d fermi-hubbard system, Science **357**, 1385 (2017), http://science.sciencemag.org/content/357/6358/1385.full.pdf.

[75] T. A. Hilker, G. Salomon, F. Grusdt, A. Omran, M. Boll, E. Demler, I. Bloch, and C. Gross, Revealing hidden antiferromagnetic correlations in doped hubbard chains via string correlators, Science **357**, 484 (2017), http://science.sciencemag.org/content/357/6350/484.full.pdf.

[76] A. Mazurenko, C. S. Chiu, G. Ji, M. F. Parsons, M. Kanász-Nagy, R. Schmidt, F. Grusdt, E. Demler, D. Greif, and M. Greiner, A cold-atom fermi-hubbard antiferromagnet, Nature **545**, 462 (2017).

[77] C. Gross and I. Bloch, Quantum simulations with ultracold atoms in optical lattices, Science **357**, 995 (2017), http://science.sciencemag.org/content/357/6355/995.full.pdf.

[78] S. Scherg, T. Kohlert, J. Herbrych, J. Stolpp, P. Bordia, U. Schneider, F. Heidrich-Meisner, I. Bloch, and M. Aidelsburger, Nonequilibrium mass transport in the 1d fermi-hubbard model, Phys. Rev. Lett. **121**, 130402 (2018).

[79] G. Salomon, J. Koepsell, J. Vijayan, T. A. Hilker, J. Nespolo, L. Pollet, I. Bloch, and C. Gross, Direct observation of incommensurate magnetism in hubbard chains, Nature **565**, 56 (2019).

[80] M. A. Nichols, L. W. Cheuk, M. Okan, T. R. Hartke, E. Mendez, T. Senthil, E. Khatami, H. Zhang, and M. W. Zwierlein, Spin transport in a mott insulator of ultracold fermions, Science **363**, 383 (2019), http://science.sciencemag.org/content/363/6425/383.full.pdf.

[81] C. S. Chiu, G. Ji, A. Bohrdt, M. Xu, M. Knap, E. Demler, F. Grusdt, M. Greiner, and D. Greif, String patterns in the doped hubbard model, Science **365**, 251 (2019).

[82] J. Koepsell, J. Vijayan, P. Sompet, F. Grusdt, T. A. Hilker, E. Demler, G. Salomon, I. Bloch, and C. Gross, Imaging magnetic polarons in the doped fermi–hubbard model, Nature **572**, 358 (2019).

[83] N. Bulut, D. J. Scalapino, and S. R. White, One-electron spectral weight of the doped two-dimensional hubbard model, Phys. Rev. Lett. **72**, 705 (1994).

[84] R. Preuss, W. Hanke, and W. von der Linden, Quasiparticle dispersion of the 2d hubbard model: From an insulator to a metal, Phys. Rev. Lett. **75**, 1344 (1995).

[85] R. Preuss, W. Hanke, C. Gröber, and H. G. Evertz, Pseudogaps and their Interplay with Magnetic Excitations in the doped 2D Hubbard Model, Phys. Rev. Lett. **79**, 1122 (1997).

[86] C. Gröber, R. Eder, and W. Hanke, Anomalous low-doping phase of the hubbard model, Phys. Rev. B **62**, 4336 (2000).

[87] S. R. White, Density matrix formulation for quantum renormalization groups, Phys. Rev. Lett. **69**, 2863 (1992).

[88] S. R. White, Density-matrix algorithms for quantum renormalization groups., Phys. Rev. B **48**, 10345 (1993).

[89] P. Corboz, S. R. White, G. Vidal, and M. Troyer, Stripes in the two-dimensional t-j model with infinite projected entangled-pair states, Phys. Rev. B **84**, 041108(R) (2011).

[90] P. Corboz, T. M. Rice, and M. Troyer, Competing states in the t-j model: Uniform d-wave state versus stripe state, Phys. Rev. Lett. **113**, 046402 (2014).

[91] P. Corboz, Improved energy extrapolation with infinite projected entangled-pair states applied to the two-dimensional hubbard model, Phys. Rev. B **93**, 045116 (2016).

[92] B.-X. Zheng, C.-M. Chung, P. Corboz, G. Ehlers, M.-P. Qin, R. M. Noack, H. Shi, S. R. White, S. Zhang, and G. K.-L. Chan, Stripe order in the underdoped region of the two-dimensional hubbard model, Science **358**, 1155 (2017), https://www.science.org/doi/pdf/10.1126/science.aam7127.

[93] E. Yusuf, A. Joshi, and K. Yang, Spin waves in antiferromagnetic spin chains with long-range interactions, Phys. Rev. B **69**, 144412 (2004).

[94] N. Laflorencie, I. Affleck, and M. Berciu, Critical phenomena and quantum phase transition in long range heisenberg antiferromagnetic chains, Journal of Statistical Mechanics: Theory and Experiment **2005**, P12001 (2005).

[95] A. W. Sandvik, Ground states of a frustrated quantum spin chain with long-range interactions, Phys. Rev. Lett. **104**, 137204 (2010).

[96] Y. Tang and A. W. Sandvik, Quantum monte carlo studies of spinons in one-dimensional spin systems, Phys. Rev. B **92**, 184425 (2015).

[97] L. Yang and A. E. Feiguin, From deconfined spinons to coherent magnons in an antiferromagnetic Heisenberg chain with long range interactions, SciPost Phys. **10**, 110 (2021).

[98] S. Yang, D.-X. Yao, and A. W. Sandvik, Deconfined quantum criticality in spin-1/2 chains with long-range interactions (2020), arXiv:2001.02821 [physics.comp-ph].

[99] L. Yang, P. Weinberg, and A. E. Feiguin, Quantum criticality in antiferromagnetic quantum spin ladders with long-range interactions (2020), arXiv:2012.14908 [cond-mat.str-el].

[100] M. Ogata, M. U. Luchini, S. Sorella, and F. F. Assaad, Phase diagram of the one-dimensional t-j model, Phys. Rev. Lett. **66**, 2388 (1991).

[101] A. Moreno, A. Muramatsu, and S. R. Manmana, Ground-state phase diagram of the one-dimensional t-j model, Phys. Rev. B **83**, 205113 (2011).

[102] R. Eder and Y. Ohta, One-dimensional $t-j$ model with next-nearest-neighbor hopping: Breakdown of the luttinger liquid, Phys. Rev. B **56**, R14247 (1997).

[103] H. Schulz, The metal-insulator transition in one-dimension (1994), 9412036 [cond-mat.str-el].

[104] A. L. Chernyshev and P. W. Leung, Holes in the $t-J_z$ model: A diagrammatic study, Phys. Rev. B **60**, 1592 (1999).

[105] A. L. Chernyshev, A. H. Castro Neto, and A. R. Bishop, Metallic stripe in two dimensions: Stability and spin-charge separation, Phys. Rev. Lett. **84**, 4922 (2000).

[106] C. D. Batista and G. Ortiz, Quantum phase diagram of the $t-J_z$ chain model, Phys. Rev. Lett. **85**, 4755 (2000).

[107] A. L. Chernyshev, S. R. White, and A. H. Castro Neto, Stripe as an effective one-dimensional band of composite excitations, Phys. Rev. B **65**, 214527 (2002).

[108] A. L. Chernyshev and R. F. Wood, Spin polarons and high-tc superconductivity, in *Models and Methods of High-Tc Superconductivity: Some Frontal Aspects*, Vol. 1, edited by J. K. Srivastava and S. M. Rao (Nova Science Publishers, Inc., Hauppauge NY, 2003) Chap. 11.

[109] J. Šmakov, A. L. Chernyshev, and S. R. White, Spinon-holon interactions in an anisotropic $t-j$ chain: A comprehensive study, Phys. Rev. B **76**, 115106 (2007).

[110] J. Šmakov, A. L. Chernyshev, and S. R. White, Binding of holons and spinons in the one-dimensional anisotropic $t-j$ model, Phys. Rev. Lett. **98**, 266401 (2007).

[111] K. Bieniasz, P. Wrzosek, A. M. Oles, and K. Wohlfeld, From "Weak" to "Strong" Hole Confinement in a Mott Insulator, SciPost Phys. **7**, 66 (2019).

[112] P. Wrzosek and K. Wohlfeld, Hole in the two-dimensional ising antiferromagnet: Origin of the incoherent spectrum, Phys. Rev. B **103**, 035113 (2021).

[113] F. Grusdt, M. Kánasz-Nagy, A. Bohrdt, C. S. Chiu, G. Ji, M. Greiner, D. Greif, and E. Demler, Parton theory of magnetic polarons: Mesonic resonances and signatures in dynamics, Phys. Rev. X **8**, 011046 (2018).

[114] F. Grusdt and L. Pollet, F_2 parton phases in the mixed-dimensional $t-J_z$ model, Phys. Rev. Lett. **125**, 256401 (2020).

[115] S. R. White and A. E. Feiguin, Real-time evolution using the density matrix renormalization group, Phys. Rev. Lett. **93**, 076401 (2004).

[116] A. J. Daley, C. Kollath, U. Schollwöck, , and G. Vidal, J. Stat. Mech.: Theor. Exp. , P04005 (2004).

[117] A. E. Feiguin, The density matrix renormalization group method and its time-dependent variants, in *XV Training Course in the Physics of Strongly Correlated Systems*, Vol. 1419 (AIP Proceedings, 2011) p. 5.

[118] S. Paeckel, T. Köhler, A. Swoboda, S. R. Manmana, U. Schollwöck, and C. Hubig, Time-evolution methods for matrix-product states, Annals of Physics **411**, 167998 (2019).

[119] A. E. Feiguin and D. A. Huse, Spectral properties of a partially spin-polarized one-dimensional hubbard/luttinger superfluid, Phys. Rev. B **79**, 100507(R) (2009).

[120] A. Nocera, F. H. L. Essler, and A. E. Feiguin, Finite-temperature dynamics of the mott insulating hubbard chain, Phys. Rev. B **97**, 045146 (2018).

[121] A. E. Feiguin and S. R. White, Time-step targeting methods for real-time dynamics using the density matrix renormalization group, Phys. Rev. B **72**, 020404(R) (2005).

[122] H. Suzuura and N. Nagaosa, Spin-charge separation in angle-resolved photoemission spectra, Phys. Rev. B **56**, 3548 (1997).

[123] M. Brunner, F. F. Assaad, and A. Muramatsu, Single-hole dynamics in the $t-j$ model on a square lattice, Phys. Rev. B **62**, 15480 (2000).

[124] G. Martinez and P. Horsch, Spin polarons in the t-j model, Phys. Rev. B **44**, 317 (1991).

[125] Z. Liu and E. Manousakis, Dynamical properties of a hole in a heisenberg antiferromagnet, Phys. Rev. B **45**, 2425 (1992).

[126] P. Horsch and A. Ramšak, Spin-polaron wave function for a single hole in an antiferromagnet, Journal of Low Temperature Physics **95**, 343 (1994).

[127] G. F. Reiter, Self-consistent wave function for magnetic polarons in the t-j model, Phys. Rev. B **49**, 1536 (1994).

[128] F. Lema and A. A. Aligia, Quasiparticle photoemission intensity in doped two-dimensional quantum antiferromagnets, Phys. Rev. B **55**, 14092 (1997).

[129] A. E. Trumper, C. J. Gazza, and L. O. Manuel, Quasiparticle vanishing driven by geometrical frustration, Phys. Rev. B **69**, 184407 (2004).

[130] I. J. Hamad, A. E. Trumper, A. E. Feiguin, and L. O. Manuel, Spin polaron in the J_1-J_2 heisenberg model, Phys. Rev. B **77**, 014410 (2008).

[131] I. J. Hamad, L. O. Manuel, and A. E. Trumper, Effects of semiclassical spiral fluctuations on hole dynamics, Phys. Rev. B **85**, 024402 (2012).

[132] I. J. Hamad, L. O. Manuel, and A. A. Aligia, Generalized one-band model based on zhang-rice singlets for tetragonal cuo, Phys. Rev. Lett. **120**, 177001 (2018).

[133] C. L. Kane, P. A. Lee, and N. Read, Motion of a single hole in a quantum antiferromagnet, Phys. Rev. B **39**, 6880 (1989).

[134] M. Valiente and D. Petrosyan, Two-particle states in the Hubbard model, J. Phys. B At. Mol. Opt. Phys. **41**, 161002 (2008).

[135] M. Valiente and D. Petrosyan, Scattering resonances and two-particle bound states of the extended Hubbard, J. Phys. B At. Mol. Opt. Phys. **42**, 121001 (2009).

[136] J.-P. Nguenang and S. Flach, Fermionic bound states on a one-dimensional lattice, Phys. Rev. A **80**, 015601 (2009).

[137] X. Qin, Y. Ke, X. Guan, Z. Li, N. Andrei, and C. Lee, Statistics-dependent quantum co-walking of two particles in one-dimensional lattices with nearest-neighbor interactions, Phys. Rev. A **90**, 062301 (2014).

[138] C. D. E. Boschi, E. Ercolessi, L. Ferrari, P. Naldesi, F. Ortolani, and L. Taddia, Bound states and expansion dynamics of interacting bosons on a one-dimensional lattice, Phys. Rev. A **90**, 043606 (2014).

[139] R. Rausch and M. Potthoff, Multiplons in the two-hole excitation spectra of the one-dimensional Hubbard model, New J. Phys. **18**, 023033 (2016).

[140] R. Rausch and M. Potthoff, Filling-dependent doublon dynamics in the one-dimensional Hubbard model, Phys. Rev. B **95**, 045152 (2017).

[141] C. Yang and A. E. Feiguin, Excitonic density waves, biexcitons, and orbital-selective pairing in two-orbital

correlated chains, Phys. Rev. B **98**, 035128 (2018).

[142] C. Dahnken, M. Aichhorn, W. Hanke, E. Arrigoni, and M. Potthoff, Variational cluster approach to spontaneous symmetry breaking: The itinerant antiferromagnet in two dimensions, Phys. Rev. B **70**, 245110 (2004).

[143] C. Gröber, R. Eder, and W. Hanke, Anomalous low-doping phase of the hubbard model, Phys. Rev. B **62**, 4336 (2000).

[144] I. J. Hamad, L. O. Manuel, and A. A. Aligia, Magnon-assisted dynamics of a hole doped in a cuprate superconductor, Phys. Rev. B **103**, 144510 (2021).

[145] H.-H. Lin, L. Balents, and M. P. A. Fisher, Exact so(8) symmetry in the weakly-interacting two-leg ladder, Phys. Rev. B **58**, 1794 (1998).

[146] Y. Tian and S. R. White, Matrix product state recursion methods for computing spectral functions of strongly correlated quantum systems, Phys. Rev. B **103**, 125142 (2021).

[147] S. R. White, D. J. Scalapino, and S. A. Kivelson, One hole in the two-leg $t-j$ ladder and adiabatic continuity to the noninteracting limit, Phys. Rev. Lett. **115**, 056401 (2015).

[148] C. Yang and A. E. Feiguin, Spectral function of mott-insulating hubbard ladders: From fractionalized excitations to coherent quasiparticles, Phys. Rev. B **99**, 235117 (2019).

[149] R. Konik, F. Lesage, A. W. W. Ludwig, and H. Saleur, Two-leg ladders and carbon nanotubes: Exact properties at finite doping, Phys. Rev. B **61**, 4983 (2000).